Fusion Engineering and Design 215 (2025) 114948

Contents lists available at ScienceDirect

Fusion Engineering and Design

journal homepage: www.elsevier.com/locate/fusengdes

Characterization of a new ^{4}He scintillator detector prototype for the ITER Radial Neutron Camera

S. Cesaroni [a,*], D. Marocco [a], V. Anagnostopoulou [c], F. Belli [a], A. Colangeli [a], N. Fonnesu [a], S. Loreti [a], F. Moro [a], G. Pagano [a], E. Pirovano [b], F. Pompili [a], M. Pontesilli [a], A. Zimbal [b], B. Esposito [a]

[a] ENEA CR Frascati, Nuclear Department, via Enrico Fermi 45, 00044 Frascati, Roma, Italy
[b] Physikalisch-Technische Bundesanstalt, Bundesallee 100, D-38116 Braunschweig, Germany
[c] "Tor Vergata" University of Rome, Industrial Engineering Department, via del Politecnico 1, 00133 Roma, Italy

ARTICLE INFO

Keywords:
ITER
Radial neutron camera
^{4}He detector
Neutron detector

ABSTRACT

In ITER, the reconstruction of the neutron emissivity profile along radial Lines-Of-Sight (LOS) is performed with the Radial Neutron Camera (RNC) diagnostic system. Neutrons produced in the plasma core through D(d, n)^{3}He and T(d, n)^{4}He reactions are measured by the RNC Ex-Port subsystem using three different types of detectors located within modules positioned at the end of each LOS collimator: a plastic scintillator, a ^{4}He gas scintillator and a single-crystal diamond matrix.

Considering plasma scenarios foreseen in ITER, measurements during full-power operations rely on the ^{4}He scintillator detector. A new prototype of this device, specifically designed for the ITER RNC system, has been developed and experimentally characterized. This work presents the results of the measurements performed at the Physikalisch-Technische Bundesanstalt (PTB) Ion Accelerator Facility (PIAF) in Braunschweig, focusing on the detector's response to different neutron energies, and at ENEA Frascati Neutron Generator (FNG), where its performance under high neutron fluxes was studied. The new ^{4}He scintillator detector prototype has proven to be suitable for its installation in the ITER RNC Ex-Port detector modules, and capable of reliable operation during the full-power scenarios of ITER operation.

1. Introduction

The ITER Radial Neutron Camera (RNC) [1] is a diagnostic system located in Equatorial Port #1 with the main objective of reconstructing the neutron emissivity profile along Lines-Of-Sight (LOS) that view the plasma radially. Uncollided 2.5 MeV and 14 MeV neutrons, produced in the plasma core by D-D and D-T reactions respectively, are measured by the RNC Ex-Port subsystem, which consists of 16 collimated LOS.

The strategy for the selection of RNC Ex-port detectors is that of having a detector set covering the whole range of D-T ITER neutron emission with some redundancy and at least one detector allowing the reconstruction of the neutron emissivity profile within ITER requirements in any given plasma scenario.

Plastic scintillators and single-Crystal Diamond (sCD) represent well-established detection techniques, widely used in nowadays tokamak experiments: their efficiency can be varied in a wide range by adapting the detector thickness.

Plastic scintillators pose radiation resistance issues over ITER lifetime and therefore they are better suited for low power D-T operation (mainly in the first phase of ITER lifetime). A 15 mm length × 15 mm diameter EJ-276 G plastic scintillator has been selected for the Ex-port RNC. This detector can be operated with a high energy threshold (10 MeV of neutron energy) and therefore with high Signal to Noise ratio (S/R) ~170 for central Ex-port RNC LOS from low power D-T scenarios up to 250 MW fusion power.

On the other hand, small thickness sCD can withstand the radiation levels expected over ITER lifetime and their use is recommended since it enables cross-checks with the other RNC subsystem (i.e. RNC In-Port) which is located inside the port plug and also hosts several sCD. A sCD matrix with 4 pixels (4 mm x 4 mm x 100 μm each) has been selected, the number of pixels being driven by cost. This detector can be operated in the ITER RNC within a fusion power range of 500 to 900 MW. However,

* Corresponding author.
E-mail addresses: silvia.cesaroni@uniroma2.it, silvia.cesaroni@enea.it (S. Cesaroni).

https://doi.org/10.1016/j.fusengdes.2025.114948
Received 17 January 2025; Received in revised form 5 March 2025; Accepted 7 March 2025
Available online 10 March 2025

a low energy threshold (3.5 MeV of neutron energy) must be used in order to have enough counting statistics, resulting in a lower S/R (~40).

The low sCD S/R and the need of detector redundancy at 500 MW fusion power for investment protection call for the use of a second detector for high power operation. A ^{4}He detector has been selected since it does not have radiation resistance problems, and its efficiency can be tuned to match counting requirements at 500 MW just by selecting the proper gas pressure. The ^{4}He detector, with a gas pressure of 80 bar, can be operated with a 6.2 MeV neutron energy threshold (S/R ~75) from 250 MW to 500 MW.

The ^{4}He scintillator has been specifically developed by Arktis Radiation Detectors Ltd [2] for the ITER RNC project. The pressurized ^{4}He detector types manufactured by Arktis have been in the market for over 10 years and according to the manufacturer no efficiency degradation has been observed so far.

The tests performed on a first prototype of the ^{4}He detector (operating at 150 bar) demonstrated its reliable neutron flux detection capabilities [3]. The integration of this device inside the detector modules of the Ex-Port RNC required modifications that led to the design and development of a second prototype. In particular, the most significant amendments consist in:

- selection of a smaller photomultiplier tube (PMT) with a low sensitivity to magnetic field
- optimization of the position of the filling gas valve and integration of a relief valve for safety reasons
- reduction of the active volume size to limit the sensitivity to scattered neutron background and the dependence of the detector response on the irradiation position
- integration of an optical fiber to transmit a light source signal to control and correct gain variation of the PMT at high count rate
- reduction of the detector operating pressure to adapt the sensitivity to the expected neutron fluence rate and limit the number of pile-up events at high count rate.

The design of the new ^{4}He scintillator detector is presented in Section 2. Experimental tests aimed at characterizing the prototype were carried out at two neutron irradiation facilities using the setup parameters indicated in Section 3. The response of the detector prototype was investigated by studying the linearity in neutron energy (Section 3.1) and count rate (Section 3.2). A discussion of the obtained experimental results and conclusions of this study are provided respectively in Section 4 and Section 5.

2. Design of the new ^{4}He scintillator detector

The new ^{4}He scintillator (Fig. 1) is a fast neutron detector with main specifications listed in Table 1. The active volume consists of a reflective and wavelength-shifting cylindrical pressure cell filled with a mixture of ^{4}He and noble gases (undisclosed by the producer), pressurized to 80 bar. Photons produced inside the active volume are seen through an optical sapphire window and detected by a PMT, which converts them into electrical pulses. The PMT is a Hamamatsu Integral Assembly (model H6153–70-Y002), resistant to strong magnetic fields and equipped with the synthetic silica type PMT R6149, which exhibits no variations in performance after irradiation with gamma rays up to 200 kGy and neutrons up to 1.4×10^{14} 1/cm^2 [4,5]. The PMT magnetic shielding consists of two cylindrical concentric layers: the internal one is made of μ-metal (relative magnetic permeability μ_1=60,000, saturation 0.8 T) and the external one made of Radiometal (relative magnetic permeability μ_2=6000, saturation 1.6 T). The design considers a magnetic field of 200 mT outside the magnetic shield (namely the expected ITER environmental field at that location) and a target residual magnetic field at the PMT of 0.1 mT. At such residual field, whatever the orientation of the PMT is with respect to the magnetic field, the PMT gain variation is negligible [4]. In order to monitor the PMT gain stability during detector operation, a radiation-hardened optical fiber able to transmit a reference light source signal to the PMT photocathode has been mounted inside the device. This layout allows the light signal source to be located far from the detector.

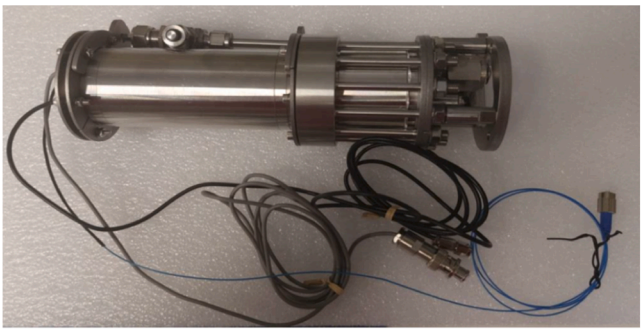

Fig. 1. The new ^{4}He scintillator detector prototype.

Table 1
Main characteristics of the new ^{4}He scintillator detector.

Detector	80 bar ^{4}He noble gas scintillator
Active volume	50 cm3
Operational temperature range	0 °C – 50 °C
PMT type	Hamamatsu H6153–70
Maximum supply voltage	+2300 V
Output range	−200 mV to 0 mV with HV=+2100 V
HV connector	SHV male
Signal connector	SMA male
Optical fiber connector	FC female
Weight	~1.7 kg
Dimensions	ca. 242 mm x 85 mm x 70 mm

3. Characterization of the detector prototype

The experimental characterization of the prototype was conducted operating the detector with high voltage of +2100 V in a standard temperature and pressure environment. Tests were performed with monoenergetic neutrons at two irradiation facilities:

- PTB Ion Accelerator Facility (PIAF, in Germany [6]), where it was possible to investigate the energy dependence of the detector's response in a so-called neutron reference field, i.e. minimizing the disturbances due to neutrons-matter interaction
- ENEA Frascati Neutron Generator (FNG, in Italy [7]), where it was possible to study the detector's behaviour under high 14.8 MeV neutron fluxes.

The detector signals were amplified 5x using a Phillips Scientific QUAD DC-300 MHz amplifier (model 771) before being acquired by the ENEA 400 MSamples/s digital acquisition system [8]. This choice allowed to cover the full ADC input dynamic range of ±1 V during measurements performed under 14.8 MeV neutron irradiation. Data were processed using a dedicated pulse shape discrimination software [9], which performs pulse detection, pulse integration to calculate the deposited energy, and pulse shape discrimination. Pulses with different decay time constants are separated by a digital equivalent of the charge comparison method, i.e. by evaluating the ratio of two values of the pulse integral (I) calculated using different time intervals starting from the peak of the pulse (called *short-gate* and *long-gate*).

3.1. Linearity in neutron energy

The linearity of the new ^{4}He scintillator detector response to neutrons of different energies was studied through experimental tests

performed at PIAF. The prototype was placed at 1.1 m distance from the neutron source with the active volume of the detector positioned under 0° relative to the incoming ion beam hitting the target. Measurements have been performed in two experimental layouts:

- Free Field (FF) configuration, in which there are no obstacles between the neutron beam and the active volume of the detector;
- Collimated Beam (CB) configuration, in which the neutron beam crosses a collimator before reaching the active volume of the detector (Fig. 2). The collimator has been specifically designed to reproduce the beam conditions of an ITER RNC collimated LOS [3]. Each test conducted using this experimental layout requires a two-step irradiation procedure:
  1. A first measurement performed with the collimator placed between the detector active volume and the neutron beam, with the collimator cavity open and perfectly aligned with both of them;
  2. A second measurement performed with the collimator cavity fully obstructed by an additional tube to determine the background contribution due to scattered neutrons.

  The second measurement must be subtracted from the first one to obtain the net signal corresponding to the almost uncollided neutron beam impinging on the detector in CB configuration.

The investigation of the detector response was carried out using four different mono-energetic neutron beams, produced through reactions listed in Table 2. The kinematics of neutron elastic scattering process determines the maximum energy transferred on recoil ^{4}He nucleus (E_{max}), which depends on the nucleus mass (A) and the energy of the neutron beam (E_n), as described by the well-known formula [10]:

$$E_{max} = \frac{4A}{(1+A)^2}E_n \quad (1)$$

During measurements performed with the neutron beam of the highest energy (14.8 MeV), up to approximately 9.5 MeV can be transferred to the ^{4}He recoil nucleus, whose range within the investigated gas mixture ensures that this energy is fully deposited inside the detector's active volume and converted into emitted light.

Fig. 3 shows the neutron Pulse Height Spectra (PHS) acquired in FF configuration and normalized to the neutron fluence for each investigated energy of the neutron beam. For each curve, it is possible to see the *recoil edge* at the highest filled ADC channels, which corresponds to the maximum energy transfer, i.e. the maximum light output emitted by the scintillating gas mixture due to the interaction of the ^{4}He recoil nuclei within the detector.

Measurements with the same energies were performed in CB configuration (Fig. 4a). As mentioned above, it was possible to isolate the background contribution and obtain the PHS related to the uncollided neutron beam, for which the recoil edge appears sharper, as expected.

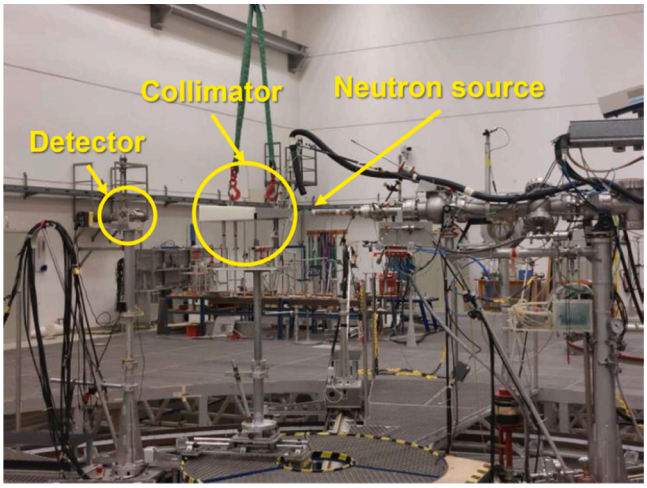

Fig. 2. The experimental setup of the Collimated Beam configuration at PIAF.

Table 2
Mono-energetic neutron beams used at PIAF to study the detector's response.

Neutron energy (MeV)	Nuclear reaction	^{4}He recoil nucleus maximum energy (MeV)
1.5	T(p, n)^{3}He	0.960
2.5	T(p, n)^{3}He	1.600
6.8	D(d, n)^{3}He	4.352
14.8	T(d, n)^{4}He	9.472

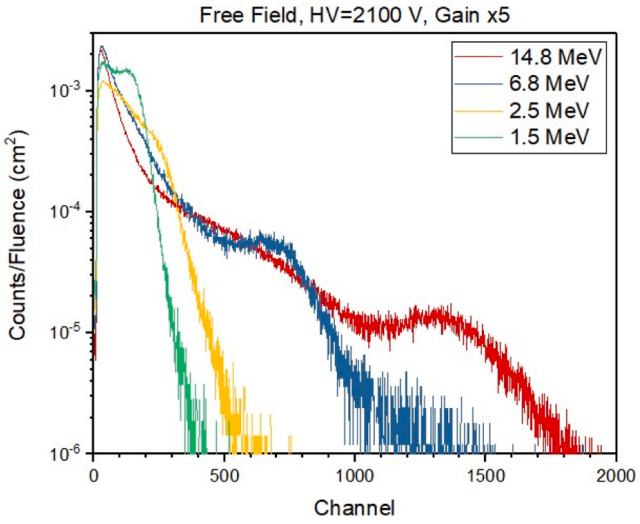

Fig. 3. PHS acquired by the detector prototype in Free Field configuration and normalized to the neutron fluence.

For the investigation of the detector response linearity with neutron energy, the recoil edge peaks were fitted using a Gaussian curve and the recoil edge channel position was conventionally set as the amplitude at half-height of the curve. As a result, the detector exhibits a perfect linearity in neutron energy (Fig. 4b).

The neutron/gamma-ray discrimination capabilities of the detector are presented in Fig. 5a which shows the discrimination plot obtained for a 14.8 MeV neutron measurement performed at PIAF. This plot was generated using *short* and *long gates* of 7.5 ns and 25 ns, respectively. The typical shapes of neutron and gamma-ray signals are shown in Fig. 5b. The results indicate that the detector is able to distinguish between neutrons and gamma-rays above channel ~160 (marked by the pink line in Fig. 5a), corresponding to the maximum energy deposited by ~1.3 MeV neutrons within the detector active volume. Above this threshold, the estimated fraction of the scattered radiation recorded in the geometry with the open collimator is 35 %.

3.2. Linearity in count rate

Further tests were performed with the aim of studying the linearity of the detector count rate in the range of 14.8 MeV neutron fluxes expected in the ITER RNC. Experiments were carried out at PIAF for neutron fluxes up to 4.1×10^6 1/(cm^{2}s) and at FNG for neutron fluxes up to 1.4×10^8 1/(cm^{2}s), in FF configuration for both irradiation facilities.

At PIAF, the 14.8 MeV neutron flux was varied by varying the distance of the detector from the beam target. The neutron flux impinging on the detector is measured experimentally based on the measurement of the accelerator current and using scaling factors for the distance correction. The measurement results are shown in Fig. 6, where both the

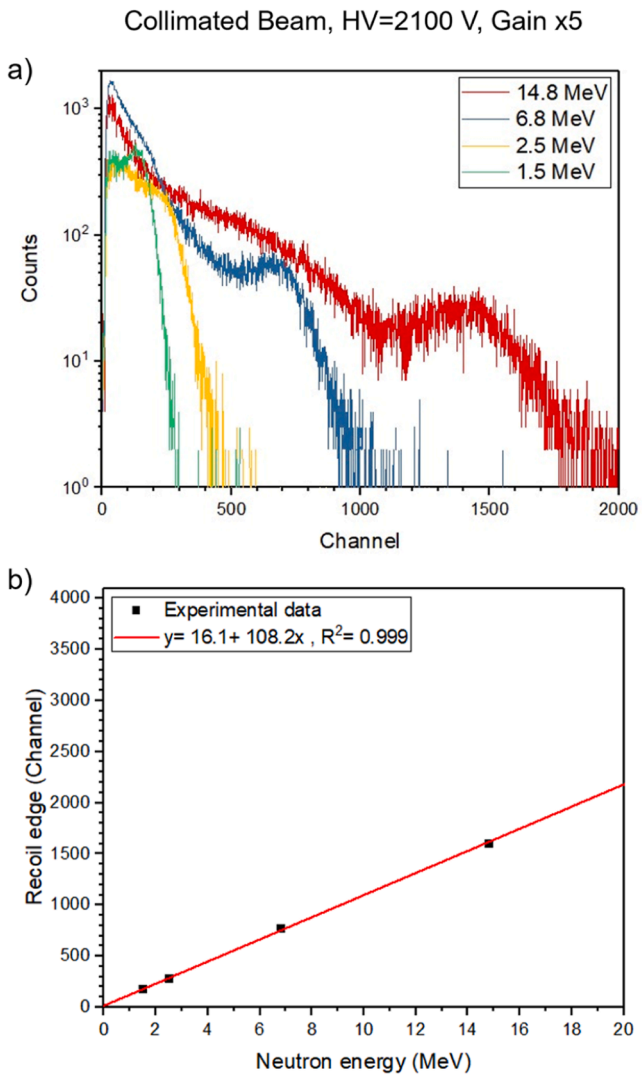

Fig. 4. (a) PHS acquired by the detector prototype in Collimated Beam configuration, and (b) the neutron energy linearity curve.

total count rate (due to neutrons, gamma rays and pile-up events) and the count rate of neutron events versus the neutron flux is reported. A deviation from linearity of the neutron count rate is observed when this count rate exceeds ~ 10^5 counts per second (cps) but linearity is recovered by taking into account of piled-up events i.e. by multiplying the count rate of neutron single events by the pile-up correction factor defined by the formula:

$$p_{CF} = 1 + \frac{c_P}{c_S} \tag{2}$$

Where c_p is the count rate of piled-up events, and c_s is the count rate of single events (neutrons and gamma-rays) detected by the processing software.

At FNG, the 14.8 MeV neutron flux was varied by changing the beam current. The neutron flux at the detector is calculated through MCNP simulations (statistical error <0.4 %). The result of the measurements is shown in Fig. 7. As also observed at PIAF, the detector's response increases linearly with the neutron flux up to a count rate of ~10^5 cps. Above this value, the correction factor is able to restore the linear behaviour at least up to about 4 × 10^6 cps.

4. Discussion of the results

Experimental tests performed at PIAF demonstrated that the detector's response is linear with respect to the energy of the incident neutron beam. The comparison between measurements conducted in the two different irradiation layouts showed an average FF/CB count ratio of ~12.2 ± 2.1 for all the investigated energies (Fig. 8). This value results similar to the calculated ratio of the portion of the detector's active volume intersected by the beam when collimated to the total, which is ~11, demonstrating a good collimator-beam alignment during CB configuration measurements.

Considering the position of the new ^{4}He scintillator detector within the ITER RNC system, it is important to determine the detector's efficiency in the CB configuration. Since during the tests a measurement with a calibrated reference detector at the prototype's position was not available, an estimation for 14.8 MeV-neutrons is derived by data collected with the FF configuration and considering the geometrical characteristics of the detector. The acquired data were analysed by setting a processing threshold of 2.5 MeV in order to avoid the low-energy neutron contribution. It should be noted that in the FF configuration, the neutron beam interacts with the entire active volume of the detector, whereas in the CB configuration, the beam reaches the detector positioned at the end of the collimator, which is designed and positioned in such a way that a beam with circular aperture of 11 mm diameter is realized at the detector position. The detector efficiency in CB configuration (ε_{CB}) is estimated by applying a geometric factor (g) to the efficiency calculated for FF configuration (ε_{FF}):

$$\varepsilon_{CB} = \varepsilon_{FF} \cdot g = \frac{R_{FF}}{A_{det}} \cdot \left(\frac{d_{det}}{\frac{V_{det}}{A_{det}}} \right) \tag{3}$$

The detector response (R_{FF}) is calculated as the ratio between the total counts excluding the background to the source fluence in FF configuration. Other terms of Eq. (2) are geometric quantities related to the detector active volume irradiated perpendicular to the cylinder axis (A_{det} is the cross-sectional area of the detector, d_{det} is the diameter of the gas cell and V_{det} is the volume). The values used for these parameters were provided by the detector manufacturer and are listed in Table 3. The calculated prototype's detection efficiency for the CB configuration results to be 4.25 × 10^{-3}.

It is worth noting that the mentioned calculation was conducted analytically, using approximations for the initial estimate of the neutron fluence incident on the detector and without detailed knowledge of the geometric tolerances of the detector components. Employing neutron transport codes to simulate the detector's response in the CB configuration could provide a more accurate estimation of the calculated parameters.

The efficiency value ε_{CB} can be compared with an estimate obtained by scaling the efficiency of the first detector prototype studied in [3]. In that study, the prototype featured the same gas mixture at a pressure of 150 bar, and its efficiency was rigorously determined using a calibrated reference detector placed at the same position of the prototype in CB configuration. Since the detector's efficiency varies linearly with the scintillating gas pressure [10], it is possible to approximate the efficiency ε_{CB}' of the new ^{4}He scintillator detector prototype by applying a simple scaling factor based on the pressure ratio:

$$\varepsilon'_{CB} = \left(\frac{80}{150} \right) \times 7.50 \times 10^{-3} = 4.0 \times 10^{-3} \tag{4}$$

The difference between the two efficiency values (about 6 %) gives a rough indication of the uncertainty on ε_{CB}.

Fig. 9 shows the summary of detector characterization in terms of neutron count rate, obtained by applying the pile-up correction factor to experimental data acquired at PIAF and FNG, and using a processing threshold of 3.3 MeV. In order to estimate the count rate expected when the new ^{4}He scintillator detector will be installed inside the RNC Ex-Port detector modules, the neutron flux values calculated for each LOS in ITER D-T scenarios are indicated as vertical lines in light blue for $Q = 10$

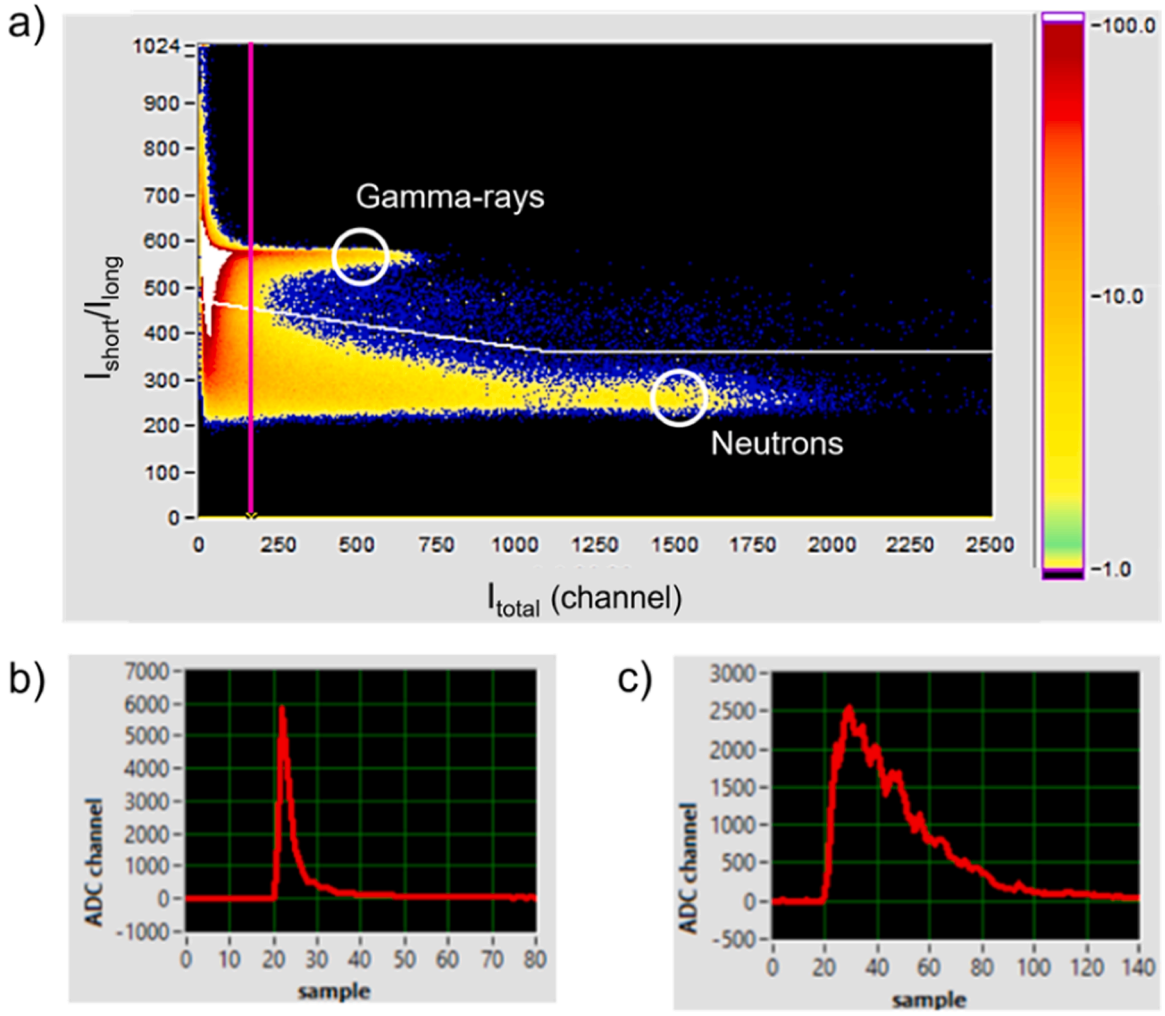

Fig. 5. Neutron/gamma-ray separation plot obtained with ^{4}He detector using a 14-MeV neutron beam at PIAF (a); Typical gamma-ray (b) and neutron (c) pulses (1 sample =2.5 ns) selected from the regions circled in white in the separation plot.

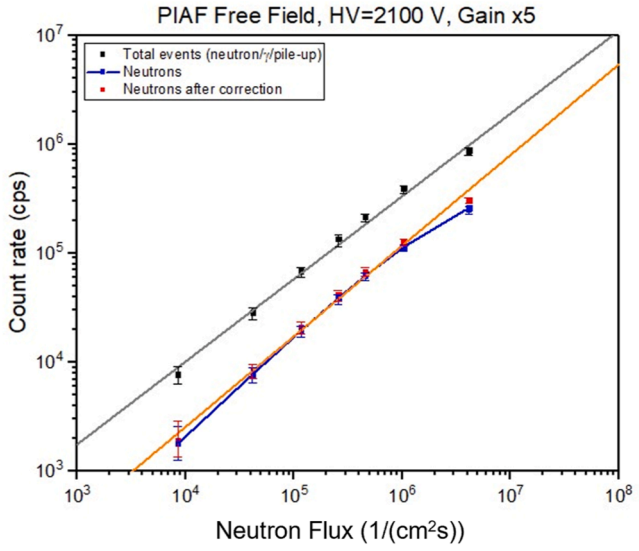

Fig. 6. Linearity of detector count rate with neutron flux at PIAF: data related to total events (black), neutrons (blue) and neutrons after applying the pile-up correction (red). Linear fits are indicated in grey for total events and orange for neutrons.

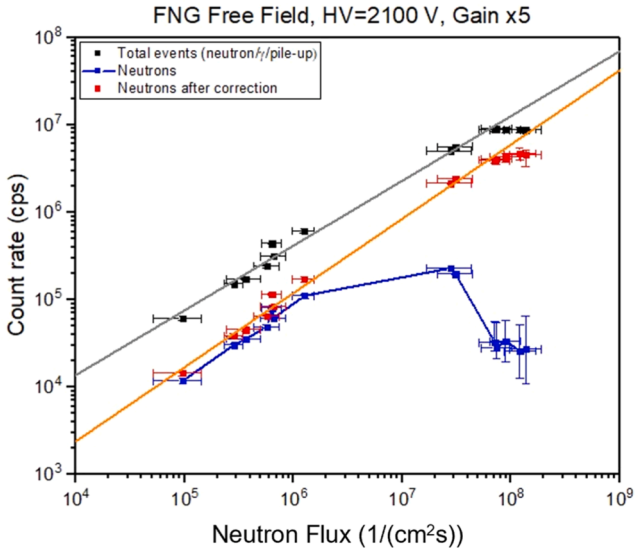

Fig. 7. Linearity of detector count rate with neutron flux at FNG: data related to total events (black), neutrons (blue) and neutrons after applying the pile-up correction (red). Linear fits are indicated in grey for total events and orange for neutrons.

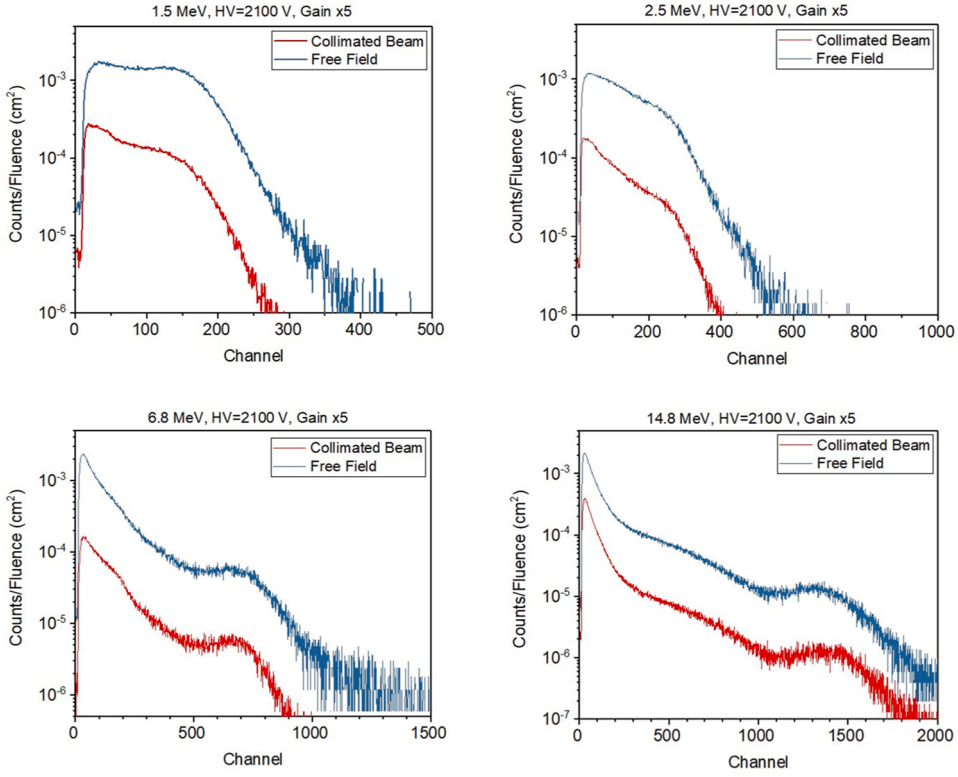

Fig. 8. Comparison between PHS acquired in FF and CB configurations, normalized to the neutron fluence for all investigated energies.

Table 3
Estimation of the detection efficiency for 14.8 MeV neutrons using a pulse height threshold corresponding to a neutron energy of 2.5 MeV.

Detector active volume			Efficiency	
Diameter (cm)	**Height (cm)**	**Volume (cm^3)**	**FF**	**CB**
4.4	3	45.6	3.34×10^{-3}	4.25×10^{-3}

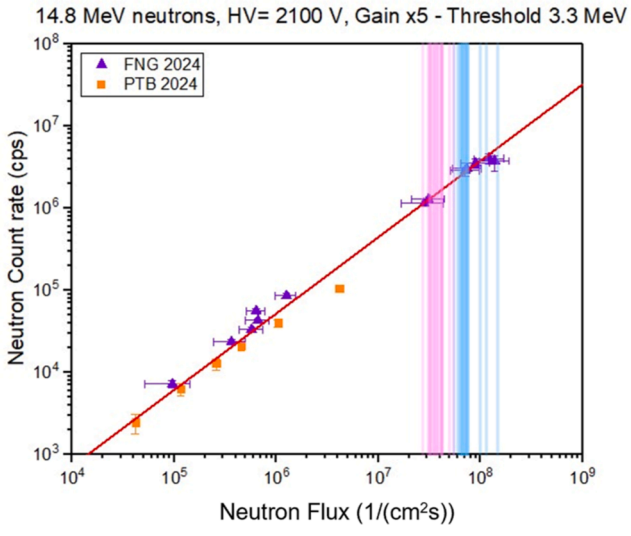

Fig. 9. Overall count rate linearity plot with neutron flux values at each RNC Ex-Port LOS detector in ITER D-T scenarios shown by vertical lines (light blue: $Q = 10$; pink: $Q = 5$).

and pink for $Q = 5$ [1]. As result, the detector's operating range accommodates these scenarios for all RNC Ex-Port LOS, except for the three outermost lines. Due to design constraints, these peripheral LOS have a shorter collimator length, resulting in a neutron flux calculated for $Q = 10$ that is too high to ensure the detector's proper response.

5. Conclusions

A new ^{4}He scintillator detector prototype designed for the ITER Ex-Port RNC has been characterized by means of experimental tests performed at PIAF and FNG with neutron beams of different energies and intensity. The detector exhibits a linear response with neutron energy, and a linearity of count rate with incoming neutron flux in the range 10^3 cps to 4×10^6 cps corresponding to 10^4 1/(cm^2s) to 7×10^7 1/(cm^2s). Application of a pile-up correction results necessary when the incoming neutron flux exceeds 10^6 1/(cm^2s) to recover the response linearity. The 14.8 MeV-neutron detection efficiency in CB configuration is experimentally determined to be $\sim 4 \times 10^{-3}$. MCNP simulations could provide a more precise assessment of this value. The detector features are considered compatible with its use in the Ex-Port RNC in $Q = 5$ and $Q = 10$ ITER D-T scenarios.

6. Disclaimer

F4E: This publication reflects only the views of the authors, Fusion for Energy cannot be held responsible for any use of the information contained therein.

ITER: The views and opinions expressed herein do not necessarily reflect those of the ITER Organization.

CRediT authorship contribution statement

S. Cesaroni: Conceptualization, Data curation, Formal analysis, Investigation, Methodology, Resources, Visualization, Writing – original draft, Writing – review & editing. **D. Marocco:** Project administration,

Software, Supervision, Validation, Visualization, Writing – review & editing. **V. Anagnostopoulou:** Validation. **F. Belli:** Conceptualization, Data curation, Methodology, Resources, Validation. **A. Colangeli:** Conceptualization, Resources. **N. Fonnesu:** Conceptualization, Resources. **S. Loreti:** Conceptualization, Resources. **F. Moro:** Conceptualization, Data curation, Formal analysis. **G. Pagano:** Resources. **E. Pirovano:** Conceptualization, Resources. **F. Pompili:** Conceptualization, Methodology, Resources. **M. Pontesilli:** Conceptualization, Methodology, Resources. **A. Zimbal:** Conceptualization, Methodology, Resources, Validation, Writing – review & editing. **B. Esposito:** Funding acquisition, Project administration, Validation, Writing – review & editing.

Declaration of competing interest

The authors declare that they have no known competing financial interests or personal relationships that could have appeared to influence the work reported in this paper.

Data availability

Data will be made available on request.

References

[1] B. Esposito, et al., Progress of design and development for the ITER radial neutron camera, J. Fusion Energy. 41 (2022) 22.
[2] https://www.arktis-detectors.com/products/neutron-detectors/.
[3] Q. Ducasse, et al., Characterization of the response and the intrinsic efficiency of a 4He scintillation detector to fast mono-energetic neutrons, Nucl. Instr. Meth. 998 (2021) 165168. A.
[4] Fine mesh PMT series for high magnetic field environments, Hamamatsu Photon. (2000).
[5] Photomultiplier Tubes Basics and Applications, Hamamatsu Photonics, 2017. Fourth edition.
[6] H.J. Brede, et al., The Braunschweig accelerator facility for fast neutron research: I. Building design and accelerators, Nucl. Instrum. Methods 169 (1980) 349.
[7] M. Martone, et al., The 14 MeV Frascati neutron generator, J. Nucl. Mater. 212 (1994) 1661.
[8] M. Riva, et al., Hardware architecture of the data acquisition and processing system for the JET neutron camera upgrade project, Fusion Eng. Des 123 (2017) 873.
[9] B. Esposito, et al., A digital acquisition and elaboration system for nuclear fast pulse detection, Nucl. Instr. And Meth., A 572 (2007) 355.
[10] G.F. Knoll, Radiation Detection and Measurement, John Wiley & Sons, 1979.